

The parameters of induced thermoluminescence of some selected phyllosilicates: a crystal defect structure study

KELLY W. LEMONS AND JAMES L. MCATEE, JR.

Department of Chemistry
Baylor University, Waco, Texas 76798

Abstract

Induced thermoluminescence of five phyllosilicates, which vary with respect to chemical composition and physical characteristics, was investigated. In addition these minerals were subjected to heating and cation fixation in order to determine the influence these processes had on induced thermoluminescence. The thermoluminescence de-excitation spectra yielded differences in glow curve intensity and electron trap activation energies as a function of clay mineral composition, charge deficiency characteristics, and type of cation fixed with the clay sample. For the sodium-exchanged montmorillonites, the induced thermoluminescence glow curve intensity was found to be proportional to the octahedral layer charge deficiency of the clay.

Both potassium and lithium-fixed samples demonstrated an increase in thermoluminescence glow curve intensity indicating that the fixation of cations on both clay surfaces and inside the crystal structure of clay minerals introduces new electron traps to the system. The increase in the number of electron traps due to potassium fixation is proportional to the degree of tetrahedral charge deficiency of the clay. This increase is proportional to the total charge deficiency of lithium-fixed montmorillonites. The average electron trap activation energy is highest for potassium-fixed clays while cation fixation and heating a given clay reduced the maximum temperature and half-width of the induced thermoluminescence glow curve. These observations are true for all the montmorillonites and hectorite studied. Nontronite demonstrates deviations from these observations which are probably due to excessive quenching of the thermoluminescence signal by iron.

Introduction

The process of thermoluminescence (TL) is effected through the release of energy in the form of light due to the recombination of "trapped electrons" and "holes" brought about by thermal activation of these charge carriers. These electron-hole centers are formed at the expense of defect centers present in crystal structures. The intensity of a TL de-excitation curve depends, therefore, primarily upon three conditions (Marfunin, 1979, p 239): (1) the number of impurities and vacancies present in the crystal structure; (2) the probability of electron-hole centers forming due to these impurities and vacancies; (3) the number of centers which do form. The presence of iron has been found to quench the TL process, reducing TL glow curve intensities (Medlin, 1968).

In quartz, impurity centers have been identified based on the valence of cations substituting for Si^{4+} . For example, electron centers (electron traps) have been identified as Ti^{3+} (*i.e.*, $\text{Ti}^{4+} + e^-$) and hole centers are designated as Al^{3+} or Fe^{3+} (Marfunin, 1979, p. 270).

An electron center ($\text{Ti}^{4+} + e^-$) is stable in the presence

of a "compensator cation M^+ " (usually H^+ , Li^+ , Na^+ , *etc.*) and unstable without such a cation (Marfunin, 1979, p. 271). Hole centers are stable without ion compensators and unstable in their presence (Marfunin, 1979, p. 271). For the case of Al^{3+} substitution for Si^{4+} in quartz, hole center stabilization is accomplished by an oxygen shared between two tetrahedra. This bridging oxygen forms an O^- center by losing one of its electrons ($\text{O}^{2-} \rightarrow \text{O}^- + e^-$), forming the complete hole center represented as O^- -Al or AlO_4^{4-} . For quartz, if the substitution is accompanied by cation compensation (H^+ , Li^+ , Na^+ , *etc.*), irradiation forms the hole center (AlO_4^{4-}) with simultaneous transformation of the compensator (M^+) to a zero valence species (Marfunin, 1979, p. 272). In the formation of a hole center due to the substitution of Al^{3+} for Si^{4+} the hole is trapped by oxygen, forming (AlO_4^{4-}) while for Fe^{3+} , hole formation in the non-bonding oxygen orbital would be unstable because of the presence of $\text{Fe}^{3+} 3d^5$ electrons in anti-bonding orbitals. Thus, FeO_4^{4-} forms at the expense of these $3d^5$ electrons, forming the center $\text{Fe}^{4+} 3d^4$ (Marfunin, 1979, p. 273).

The TL process and information contained in a TL de-excitation curve is treated in detail in a previous publica-

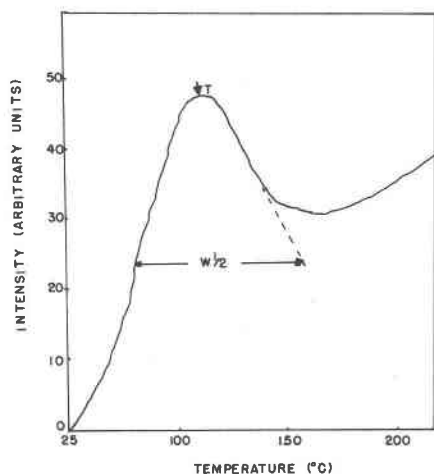


Fig. 1. Representative thermoluminescence de-excitation curve: T is the temperature at the maximum intensity of the glow curve; and $W_{.5}$ is the peak half-width at its half-height.

tion (Lemons and McAtee, 1982). In summary, TL is a three step process. The first step involves the ionization of elements in a compound by exposing it to sufficiently energetic radiation (X-rays, gamma rays, etc.). These electrons are allowed to migrate through the conduction band until exposure to radiation ceases. The second step is the trapping of some of these free electrons. Once the radiation ceases, most electrons return to a parent ion. Some are trapped, primarily by defect centers, and remain at higher energy levels. The third step is the release of these trapped electrons which is brought about by slowly raising the temperature of the sample. Once released, they again migrate until they recombine with a parent ion (hole). If this recombination is at a luminescent center, energy is released in the form of light. If recombination is at a non-luminescent center, energy is released in the form of heat (Aitken, 1974, p. 87).

The information immediately available from a TL glow curve can be classified into two categories (Fig. 1). The first is the relative number of electron-hole centers present in the sample. This is determined by the intensity or area of a TL glow curve (Fig. 1). The second category is the relative activation energy of the electron traps. This is determined by the expression (Braunlich, 1968; Marfunin, 1979, p. 229).

$$E = kT^2/W_{0.5}$$

where k is Boltzmann's constant which equals $8.62 \times 10^{-5} \text{ eVK}^{-1}$, $W_{0.5}$ is the half-width of the curve at its half-height (K), and T is the maximum temperature of the de-excitation curve (K).

The purpose of this investigation was to establish a model of the induced TL of some selected phyllosilicates which possess a range of varying chemical composition and of different physical characteristics. The physical characteristics were determined by employing cation

exchange capacity (CEC), and X-ray diffraction (XRD) methods of analysis. These procedures were also used to study the effects that heating and cation fixation had on these clay minerals.

Once these studies were concluded, the information they provided was correlated to the TL spectrum of each sample. Therefore, the effects that sample composition, heating, and cation fixation have on the TL spectra of the clay minerals was determined and accounted for.

Experimental

Sample preparation

The clays used in this investigation were obtained from the Clay Minerals Society Repository at the University of Missouri. These samples and their geographical origins are presented in Table 1 (van Olphen and Fripiat, 1979).

Each clay was dispersed in two liters of deionized water using a high speed blender. The amount of sample used was enough to produce one percent suspensions. These suspensions were allowed to settle for 48 hours in order to remove any nonclay minerals. After 48 hours, the top 1500 ml was decanted off. The remaining 500 ml contained the impurity minerals and was discarded. The hectorite sample required subsequent centrifuging to remove calcite which was of small enough size as to remain in suspension after 48 hours. Sample purity was determined by X-ray diffraction, and no crystalline impurities were found. Each sample was then treated with a sodium dithionite-sodium citrate solution buffered with sodium bicarbonate to remove any adsorbed iron (Mehra and Jackson, 1959).

Each clay was converted to its sodium form by one of two methods. The Wyoming montmorillonite and the nontronite were exchanged by adding an excess of sodium chloride to their suspensions. They were then redispersed and blended for 15 minutes in a high speed blender and allowed to age for 48 hours. Each suspension was then centrifuged and the clear supernatant solution discarded. The clays were then rinsed with deionized water and the suspension centrifuged again. Rinsing the samples in this manner was continued until no chloride ions were determined to be present in the supernatant solution. This determination was made by adding silver nitrate to the decanted clear solution. The hectorite sample and the Arizona and Texas montmorillonites were sodium exchanged by repeatedly passing them through a cation exchange column of sodium charged Dowex 50W-X8 resin. The resin was recharged with sodium after each clay was passed through the column. The temperature of the column was maintained at a temperature range of 60–70°C. The completeness of exchange for each sample was confirmed by X-ray diffraction of oriented samples on glass slides at 51 percent relative humidity.

One half of each sample in its sodium form was oven dried at 105°C and then ground to pass through a number 220 sieve. One half of this dried sample was then heated in an oven at 220°C for 24 hours. This sample was then reground to pass through a number 220 sieve. At this stage, one half of each of the original samples in their sodium form was still in suspension, one fourth had been dried at 105°C, and the remaining one fourth dried and heated at 220°C for 24 hours. These two dried portions of the clays were prepared to serve as references in order to determine what effects heating and cation fixation have on the clays.

The remaining portion of each sample still in suspension was

divided in half. One half was converted to its potassium exchanged form and the other half converted to its lithium exchanged form. This exchange was accomplished in all samples by placing an excess of potassium bromide or lithium chloride in the respective suspensions. Blending, aging, centrifuging, and rinsing were carried out as described for sodium exchange. The clays were then oven dried at 90°C and ground to pass through a number 220 sieve. For fixation of the potassium and lithium cations, the dried potassium clays were heated at 105°C for 24 hours. In summary, four samples were prepared from each of the five clays—a sodium form heated at 105°C, a sodium form heated at 220°C, a potassium form heated at 105°C (potassium fixed), and a lithium form heated at 220°C (lithium fixed).

X-ray diffraction

X-ray diffraction studies were undertaken to observe mineralogical purity, the effects heating and cation fixation had on the crystal structure of the samples, and to obtain data on the diffraction characteristics of the clay samples. All XRD studies were accomplished using a Picker X-ray Diffractometer equipped with a copper X-ray tube. Nickel foil was used to filter out the $\text{CuK}\beta$ X-rays, allowing only $\text{CuK}\alpha_1$ and $\text{K}\alpha_2$ to be used. The potential and current supplied to the X-ray tube were 40 kV and 20 mA, respectively.

X-ray diffraction patterns on randomly packed powder were made for the sodium clays heated at 105°C and equilibrated with a 51% relative humidity atmosphere in order to observe the characteristic 06 *hk* diffraction lines. Also, weighed portions of each sample (sodium, potassium, and lithium) were mixed with sufficient quantities of deionized water to prepare 0.2 percent suspensions. These suspensions were dispersed for 15 minutes using a Sonifier Cell Disrupter model #W185 at a power setting of 35 watts. Two milliliter portions of each suspension were transferred to glass slides placed on a flat, level surface and allowed to dry at approximately 60°C under an infrared lamp. These oriented samples contained equal amounts of clay covering equal areas which allowed for quantitative X-ray diffraction patterns to be obtained. Once dried, each oriented sample was placed in a 51 percent relative humidity desiccator for 48 hours and then X-rayed. X-ray diffraction patterns were obtained of each clay to determine the extent of collapse experienced due to heating and cation fixation (Table 2). After the diffraction patterns were made, each sample was placed in an ethylene glycol desiccator for 48 hours and diffraction patterns determined for these samples (Table 3). The relative intensities were calculated by taking the most intense peak (I^*) as having a 100 percent intensity and then comparing the other peaks to it.

Elemental analysis and cation exchange capacity determinations

The sodium clays prepared at 105°C were analyzed for elemental composition by quantitative energy dispersive electron probe X-ray analysis. This analysis was made using a Princeton Gamma Tech System III analyzer (PGT III) employing a SiLi detector and a Nova Scan scanning electron microscope (SEM). The accelerating voltage used with the SEM was 15 kV and the probe current was maintained at 3.0×10^{-9} A.

The PGT III provides two programs used in this study. One, the BSTAND program, is a standard processing program which calculates pure element peak intensities from the standard spectra collected. These standards may be either pure elements or multi-element standards. Another was the BSAM program which

Table 1. Description of clays investigated by thermoluminescence*

Clay	Origin	Distinguishing Characteristics [†]
Na-montmorillonite	New Castle Formation, Crook County, Wyoming	Predominantly NA exchangeable cations, CEC=76.4 meq/100 g, Si/Al=0.1/0.31. Moderately high Fe_2O_3 and MgO concentrations (3.35 and 3.05%, respectively).
Ca-montmorillonite	Manning Formation, Gonzales County, Texas	Predominately Ca exchangeable cations, CEC=84.4 meq/100 g, Si/Al=1.0/0.23. Low Fe_2O_3 concentration (0.65%) and moderately high MgO concentration (3.69%).
Ca-montmorillonite	Bidahochi Formation, Apache Arizona	Predominately Ca exchangeable cation. CEC=120 meq/100 g, Si/Al=1.0/0.29. Low Fe_2O_3 concentration (1.42%). High MgO concentration (6.46%).
hectorite	Red Mountain Andesite Formation, San Bernardino County, California	CEC=43.9 meq/100 g, Si/Al=1.0/0.02. Low Fe_2O_3 concentration (0.02%). High MgO concentration (15.3%). High CaO concentration (23.4%).
nontronite	Washington State	not listed in Data Handbook

*Samples from Source Clay Repository, The Clay Minerals Society.

†Data from van Olphen and Fripiat (1979).

Table 2. X-ray diffraction data of oriented samples equilibrated with a 51% relative humidity atmosphere

Sample	(001) line A	line-intensity ($I/I^* \times 100\%$)	symmetry*
<u>Wyoming montmorillonite</u>			
sodium form (105°C)	12.80	47.4	asymmetric (s)
sodium form (220°C)	12.62	32.9	asymmetric (b)
lithium fixed	9.60	6.6	asymmetric (b)
potassium fixed	11.94	32.9	asymmetric (b)
<u>Texas montmorillonite</u>			
sodium form (105°C)	12.62	52.6	symmetric (s)
sodium form (220°C)	12.62	55.3	asymmetric (s)
lithium fixed	9.81	2.6	- (vb)
potassium fixed	12.28	21.0	asymmetric (b)
<u>Arizona montmorillonite</u>			
sodium form (105°C)	12.62	100.0	symmetric (vs)
sodium form (220°C)	12.62	34.9	asymmetric (vs)
lithium fixed	-	-	-
potassium fixed	11.24	22.4	asymmetric (b)
<u>hectorite</u>			
sodium form 105°C)	12.27	98.7	symmetric (s)
sodium form (220°C)	12.62	73.7	symmetric (b)
lithium fixed	12.27	52.6	symmetric (b)
potassium fixed	11.94	69.7	asymmetric (vb)
<u>nontronite</u>			
sodium form (105°C)	12.62	85.5	symmetric (vs)
sodium form (220°C)	12.44	86.8	symmetric (s)
lithium fixed	12.62	23.7	symmetric (vb)
potassium fixed	11.78	23.7	symmetric (vb)

* (vs) = very sharp; (s) = sharp; (b) = broad; (vb) = very broad

Table 3. X-ray diffraction data of oriented samples equilibrated with an ethylene glycol atmosphere

Sample	(001) line λ	Symmetry*
<u>Wyoming montmorillonite</u>		
sodium form (105°C)	17.31	symmetric (s)
sodium form (220°C)	17.31	symmetric (vs)
lithium fixed	9.40	asymmetric (b)
potassium fixed	16.98	asymmetric (s)
<u>Texas montmorillonite</u>		
sodium form (105°C)	17.31	symmetric (vs)
sodium form (220°C)	17.21	symmetric (vs)
lithium fixed	9.82	asymmetric (b)
potassium fixed	16.35	asymmetric (b)
<u>Arizona montmorillonite</u>		
sodium form (105°C)	16.98	symmetric (s)
sodium form (220°C)	17.31	symmetric (s)
lithium fixed	—	—
potassium fixed	15.23	symmetric (s)
<u>hectorite</u>		
sodium form (105°C)	17.31	symmetric (vs)
sodium form (220°C)	17.31	asymmetric (s)
lithium fixed	17.31	symmetric (s)
potassium fixed	16.98	symmetric (s)
<u>nontronite</u>		
sodium form (105°C)	16.98	asymmetric (s)
sodium form (220°C)	16.98	asymmetric (s)
lithium fixed	17.66	asymmetric (b)
potassium fixed	14.72	asymmetric (vb)

* (vs) = very sharp; (s) = sharp; (b) = broad; (vb) = very broad

is a quantitative program that performs background subtraction, peak overlap corrections, and matrix corrections. Absolute quantitative analysis is obtained by the program comparing the peak intensities of the unknown compound to the intensities of the standards stored in BSTAND. All background subtraction peak overlap corrections, and matrix corrections are determined by the program FRAMEC, written by the U.S. National Bureau of Standards.

Small quantities of the samples to be analyzed were pressed

into pellets, affixed to aluminum sample stubs using conducting adhesive, and carbon coated using a Hitachi HUS-3 vacuum evaporator. The voltage applied to the carbon electrode was 13.5 V, and the vacuum was 10^{-5} torr. The clay standards N.B.S. #98A and Magcobar #5A from the U.S. National Bureau of Standards were prepared in the same manner. The standard Magcobar #5A contains a fairly high silicon to aluminum ratio (4.3:1) and moderate to high concentrations of sodium, potassium and calcium. The N.B.S. #98A standard was chosen for its moderately high titanium concentration. Spectra were collected from the standards and the data stored in the PGT III BSTAND program. From these standards, the elemental composition of the samples were determined (Table 4), and the unit cell formulas calculated (Table 5). Computation of the unit cell formulas of the samples investigated was made by the following set of assignment rules (Jackson, 1975, p. 596; van Olphan, 1977, p. 258): (1) Twenty oxygen atoms and four hydroxide ions are assigned per unit cell; (2) all of the silicon detected is allotted to the tetrahedral layer; (3) any remainder in the tetrahedral layer is filled by aluminum; (4) the remaining aluminum and all other cations (exclusive of adsorbed or exchangeable cations) are assigned to the octahedral layer.

The X-ray energy of lithium is too low (54.75 eV) to be detected by energy dispersive X-ray analysis; therefore, lithium determinations required dissolution of the samples with hydrofluoric acid, subsequent complexing of any remaining free F^- with boric acid, and analysis of the resulting solutions using Atomic Absorption Spectrophotometry (Jackson, 1975, p. 535). A Perkin Elmer model 403 Atomic Absorption Spectrophotometer was used with a wavelength setting of 335 nm.

Calculation of the cation exchange capacity (CEC) of the samples required replacement of the adsorbed cations and concentration determinations of these removed cations which have been placed in solution. Replacement of the adsorbed cations was accomplished by mixing each sample with a buffered methanol-ammonium chloride solution at a pH of 8.2 (Jackson, 1975, p. 268). Three specimens of each sample were washed with methanol-ammonium chloride solution three times and centrifuged after each washing. The washings were combined and brought to a standard volume for Atomic Absorption analysis (Table 6). The wavelength settings used for the various elements were: sodium, 295 nm; lithium, 335 nm; and potassium, 383 nm. The lithium and

Table 4. Weight percent of elements in sodium samples prepared at 105°C

	Wyoming montmorillonite	Texas montmorillonite	Arizona montmorillonite	hectorite	nontronite
SiO ₂	62.1 ± 0.2	65.9 ± 0.7	61.5 ± 0.2	59.7 ± 0.4	53.0 ± 0.2
Al ₂ O ₃	26.1 ± 0.1	22.0 ± 0.9	22.3 ± 0.1	1.7 ± 0.1	13.7 ± 0.2
TiO ₂	0.4 ± 0.0	0.3 ± 0.0	0.4 ± 0.0	0.4 ± 0.0	0.5 ± 0.0
Fe ₂ O ₃	3.9 ± 0.0	1.2 ± 0.1	2.1 ± 0.1	0.8 ± 0.1	21.9 ± 0.1
MnO	0.1 ± 0.0	0.1 ± 0.0	0.2 ± 0.0	0.2 ± 0.0	0.2 ± 0.0
MgO	2.7 ± 0.1	3.6 ± 0.4	5.5 ± 0.1	26.6 ± 0.1	1.2 ± 0.0
CaO	0.5 ± 0.0	0.7 ± 0.1	1.0 ± 0.0	0.6 ± 0.0	0.8 ± 0.0
Na ₂ O	3.9 ± 0.0	1.2 ± 0.0	4.4 ± 0.3	5.7 ± 0.4	6.7 ± 0.1
K ₂ O	0.1 ± 0.0	0.1 ± 0.0	0.1 ± 0.0	0.1 ± 0.0	0.1 ± 0.0
Li ₂ O*	---	---	---	2.66 ± 0.04	---

* Determined by AA spectrophotometry

Table 5. Unit cell formulas of sodium samples prepared at 105°C

Sample	Structural Formula
Wyoming montmorillonite	$(Si_{7.40}Al_{0.60})(Al_{3.08}Mg_{0.48}Fe_{0.37}Ti_{0.03}Mn_{0.01})_{20}(OH)_4(Na_{0.90}Ca_{0.13}K_{0.01})$
Texas montmorillonite	$(Si_{7.97}Al_{0.03})(Al_{3.03}Mg_{0.65}Fe_{0.11}Ti_{0.03}Mn_{0.02})_{20}(OH)_4(Na_{0.28}Ca_{0.09}K_{0.01})$
Arizona montmorillonite	$(Si_{7.55}Al_{0.45})(Al_{2.79}Mg_{1.01}Fe_{0.19}Ti_{0.05}Mn_{0.02})_{20}(OH)_4(Na_{1.05}Ca_{0.13}K_{0.02})$
hectorite	$(Si_{7.69}Al_{0.26})(Mg_{5.11}Li_{1.38}Fe_{0.08}Ti_{0.03}Mn_{0.02})_{20}(OH)_4(Na_{1.42}K_{0.16}Ca_{0.16})$
nontronite	$(Si_{7.07}Al_{0.93})(Fe_{2.19}Al_{1.22}Mg_{0.24}Ti_{0.05}Mn_{0.02})_{20}(OH)_4(Na_{1.74}Ca_{0.11}K_{0.02})$

potassium clays were analyzed for sodium to determine the extent of exchange. In all cases, no sodium or only trace amounts of sodium were determined, indicating essentially complete ion exchange.

Thermoluminescence

A block diagram of the equipment used in this study has been shown in a previous publication (Lemons and McAtee, 1982).

Weighed portions of each sample equilibrated with a 51% relative humidity atmosphere were mixed with a sufficient amount of silicon oil to produce a 2:1 silicon oil to clay weight ratio. Silicon oil inhibits the effects of moisture, oxygen, and light adsorption on the TL spectra (Ralph and Han, 1968). These clay-oil mixtures were then silk-screened onto squares of aluminum foil. Silk-screening of the clays provides samples with a uniform thickness and area. Sample thickness and area must remain constant since any variations produce changes in the intensity and peak position of the TL glow curve spectrum (Lemons and McAtee, 1982).

The sample pans were then placed in asbestos holders and the undersides painted with a uniform layer of a graphite suspension (Aquadag) in order to promote uniform heating of the sample.

One at a time, each sample was exposed to a dose of 436 R of tungsten X-radiation. Each clay sample was then placed in the heating stage of the TL equipment and exposed to uniformly increasing heat. The heating rate of the sample was maintained at a constant 0.893°C/sec by a DATA TRAK programmer. After each sample was heated and its TL spectrum observed the sample was discarded since heating clay samples to such high temperatures alters their chemical and physical properties, producing a different TL spectrum if the same sample is re-exposed to radiation and re-heated (Lemons and McAtee, 1982). Therefore, it was necessary to make eight samples for each clay mineral studied. One of each of the eight samples prepared was examined by TL without exposure to X-radiation in order to determine the presence of any naturally occurring TL in the clay samples. No sample exhibited any natural TL (Fig. 2).

Results and discussion

Elemental analyses and structural formulas

Table 4 lists the results of the elemental analyses of the sodium forms of the samples heated to 105°C. Nontronite

exhibits a high iron concentration and low magnesium concentration (21.9 and 1.2%, respectively). Hectorite displays a low iron and high magnesium concentration (0.8 and 26.6%, respectively). The montmorillonites possess concentrations of these two elements falling in the region between these two extremes.

Of the three montmorillonites, according to the unit cell calculations summarized in Table 5, the Arizona sample possesses the greatest amount of octahedral substitution,

Table 6. Cation exchange capacities

Sample	CEC (meq/100 g clay) ± λ
<u>Wyoming montmorillonite</u>	
sodium form (105°C)	75.58 ± 0.64
sodium form (220°C)	68.34 ± 0.52
lithium fixed	18.05 ± 1.07
potassium fixed	13.83 ± 0.51
<u>Texas montmorillonite</u>	
sodium form (105°C)	70.56 ± 0.58
sodium form (220°C)	54.38 ± 0.29
lithium fixed	9.85 ± 0.42
potassium fixed	12.79 ± 0.39
<u>Arizona montmorillonite</u>	
sodium form (105°C)	94.21 ± 0.82
sodium form (220°C)	56.31 ± 0.27
lithium fixed	8.31 ± 0.61
potassium fixed	28.03 ± 0.67
<u>hectorite</u>	
sodium form (105°C)	50.00 ± 0.21
sodium form (220°C)	48.32 ± 0.30
lithium fixed	19.75 ± 1.25
potassium fixed	12.81 ± 0.43
<u>nontronite</u>	
sodium form (105°C)	136.58 ± 1.39
sodium form (220°C)	96.65 ± 0.81
lithium fixed	7.84 ± 0.87
potassium fixed	7.20 ± 0.49

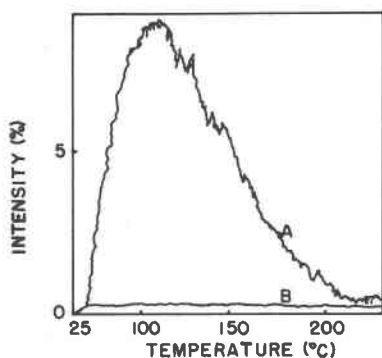


Fig. 2. Thermoluminescence de-excitation spectrum of Wyoming sodium montmorillonite prepared at 105°C: A) Induced Thermoluminescence, and B) Natural Thermoluminescence.

demonstrating a charge deficiency of 9.8×10^{-1} equivalents. The second most octahedrally-substituted montmorillonite is the Texas clay, giving an octahedral charge deficiency of 6.4×10^{-1} equivalents. The Wyoming sample is the least octahedrally charge-deficient clay, having a charge deficit of only 4.6×10^{-1} equivalents.

With respect to tetrahedral substitution, the Wyoming montmorillonite has the highest degree of substitution (6.0×10^{-1} equivalents). The Arizona montmorillonite is second with a tetrahedral deficiency of 4.5×10^{-1} equivalents, while the Texas clay exhibits substitutions in the tetrahedral layer equal to 3.0×10^{-2} equivalents.

The results of the hectorite elemental analysis and subsequent unit cell calculation (Table 5) display a high octahedral substitution (1.24 equivalents) and a low tetrahedral deficiency (2.6×10^{-1} equivalents). However, calculated values of the formula demonstrate an excess of octahedral cations present (6.2×10^{-1} equivalents excess). The magnesium value may be high due to adsorbed magnesium not removed by cation exchange. However, the most important value of the formula calculation is the high lithium cation concentration (1.38 equivalents) in the octahedral layer.

For unit cell calculations of nontronite, the iron present was assumed to be in the Fe^{3+} oxidation state. This might account for the observed fact that the formula calculation shows a low octahedral substitution (21.1×10^{-1} equivalents) while the clay demonstrates a high CEC (Table 6). This discrepancy might be explained by the presence of ferrous cations. Tetrahedral substitution is undoubtedly relatively high though exhibiting a charge deficiency of 9.3×10^{-1} equivalents.

Cation exchange capacities

The CEC determinations for the four smectites (Table 6) agree well with results calculated for unit cell formulas of the samples. The smectite with the highest CEC (nontronite) also shows the highest concentration of interlayer cations calculated for its formula (1.98 equiva-

lents), while the smectite with the lowest CEC (the Texas montmorillonite) displays the lowest interlayer cation concentration (0.47 equivalents). Hectorite deviates from a correlation of the CEC and interlayer cation concentration with its CEC giving lowest value of all samples analyzed. However, the formula calculated for hectorite displays the second highest interlayer cation concentration with respect to all the samples investigated. Therefore, it may be that incomplete exchange occurred for hectorite when displacement of interlayer cations was attempted with ammonium chloride.

X-Ray diffraction

An important aspect of powder diffraction patterns of randomly ordered clays was the observation that the 06 peak of nontronite occurred at a position inconsistent with respect to the other samples. The 06 *d*-spacing for dioctahedral clays should occur at about 1.50Å, while the 06 *d*-spacing for trioctahedral clays is around 1.53Å (Grim, 1968, p. 140). For the dioctahedral clays studied (the Wyoming, Arizona, and Texas montmorillonites) and the trioctahedral hectorite, these expected spacings were observed. However, for the nontronite clay, the 06 *d*-spacing occurred at 1.515Å. This value falls directly in the middle of the region separating the 06 peak of dioctahedral and trioctahedral clays.

X-ray diffraction of the oriented slides shows the effect that heating and cation fixation have on the structure of the samples (Tables 2 and 3). The three lithium fixed montmorillonites display complete or almost complete collapse of the 001 peak even after equilibration with both a 51% relative humidity atmosphere and with ethylene glycol. The hectorite sample was essentially unaffected by lithium fixation. Both 51% relative humidity atmosphere and ethylene glycol expanded the hectorite layers. Nontronite presented a different diffraction pattern than all the other samples. When compared to the sodium form of nontronite, it can be seen that lithium fixation did not appreciably affect the position of the 001 peak; however, the intensity of the peak was extensively reduced when the sample was equilibrated with a 51% relative humidity atmosphere. X-ray diffraction intensity measurements of lithium-fixed nontronite equilibrated with ethylene glycol were not possible because adsorption of ethylene glycol caused the sample to bubble allowing small portions of the sample to rise off the glass slide removing some of the sample from the X-ray beam.

All the potassium fixed samples equilibrated in a 51% relative humidity atmosphere showed a reduction of the 001 peak intensity as compared to the sodium samples prepared at 105°C, and peak shifts occurred toward higher angles and thus lowered *d*-values for all samples except hectorite. Potassium fixation may not have affected the hectorite sample since most of its charge deficiency occurs in the octahedral layer. Potassium fixation due to octahedral defects is of lower energy than fixed potassium cations due to tetrahedral substitution (van Olphen,

1977, p. 69) thus water vapor seems to be able to re-expand the hectorite sample. For ethylene glycol-saturated potassium fixed samples, 001 peak positions shift to higher angles for all samples indicating that postassium fixation occurs. Variations with regard to (001) peak intensities of the potassium fixed samples equilibrated with ethylene glycol could not be determined due to the raising of the sample off the glass slide. However, peak shifts to lower d values are discernable and indicate that potassium fixation takes place.

Thermoluminescence

For the sodium smectites studied, the intensity of the TL glow curves are proportional to the degree of charge deficiency in the octahedral layer (Tables 5 and 7). Arizona montmorillonite possesses the greatest octahedral charge deficiency and also the most intense TL curve. Texas montmorillonite has the second highest octahedral charge deficiency of the montmorillonites and the second most intense TL de-excitation curve. Wyoming montmorillonite has the lowest octahedral charge deficiency of the montmorillonites and also the least intense TL glow curve. Nontronite, with its very low octahedral charge deficiency (based on the assumption of Fe^{3+} substitution), has the lowest TL intensity of all the samples studied.

We propose that the sources of the freed electrons (holes) are, in most cases, the oxygens which bridge an octahedral unit containing a defect with an octahedral unit which is not deficient in positive charge. Defects can be both substitution of a cation by a cation of lower valence or the absence of a cation from an adjacent octahedral unit, as is common in the case of dioctahedral samples. This latter situation may explain the observation that hectorite (a trioctahedral clay) has such a low TL glow curve intensity even though octahedral substitution is fairly high. If the substitution of Fe^{2+} is present to a great extent in the nontronite sample, this also could explain its low TL glow curve intensity as well as its partial trioctahedral characteristics. Since dioctahedral clays are defined as clays which contain two cations in three possible octahedral sites of its unit cell (Grim, 1968, p. 86), octahedral vacancies would of course be present in each unit cell of dioctahedral clays. Trioctahedral hectorite contains a greater number of octahedral cations than dioctahedral samples, possessing therefore, a lower number of octahedral vacancies. Hence, for dioctahedral clays, a greater number of holes could be trapped at these oxygens bridging a vacant octahedral site with a non-vacant one.

Traps present in the sodium clays are proposed as existing due to anion vacancies in the clay, the formation of the SiO_4^{5-} radical, and the presence of lattice sites of excess positive charge. It is recognized that anion vacancies (*i.e.*, the absence of an oxygen from the crystal lattice) are common in other minerals and organic com-

Table 7. TL glow curve areas, maximum peak temperatures, half width, and electron trap activation energies

Samples	Glow curve areas $\pm \lambda$ (%)	$T \pm \lambda$ ($^{\circ}\text{K}$)	$W_{1/2} \pm \lambda$ ($^{\circ}\text{K}$)	$E \times 10^3 \pm \lambda$ (eV)
<u>Wyoming montmorillonite</u>				
sodium form (105 $^{\circ}\text{C}$)	9.4 \pm 0.8	380 \pm 5	106 \pm 2	1.33 \pm 0.04
sodium form (220 $^{\circ}\text{C}$)	7.9 \pm 0.2	355 \pm 6	98 \pm 3	1.27 \pm 0.03
lithium fixed	19.9 \pm 0.4	365 \pm 5	93 \pm 3	1.35 \pm 0.03
potassium fixed	18.5 \pm 1.1	368 \pm 3	93 \pm 8	1.44 \pm 0.14
<u>Texas montmorillonite</u>				
sodium form (105 $^{\circ}\text{C}$)	14.4 \pm 0.1	379 \pm 5	109 \pm 5	1.29 \pm 0.05
sodium form (220 $^{\circ}\text{C}$)	12.8 \pm 0.6	369 \pm 2	106 \pm 4	1.26 \pm 0.01
lithium fixed	22.1 \pm 0.6	370 \pm 3	110 \pm 4	1.23 \pm 0.05
potassium fixed	19.9 \pm 0.4	379 \pm 4	105 \pm 5	1.36 \pm 0.04
<u>Arizona montmorillonite</u>				
sodium form (105 $^{\circ}\text{C}$)	35.4 \pm 0.4	395 \pm 3	122 \pm 3	1.25 \pm 0.04
sodium form (220 $^{\circ}\text{C}$)	21.5 \pm 0.4	375 \pm 3	104 \pm 8	1.34 \pm 0.10
lithium fixed	100.0 \pm 5.5	374 \pm 2	104 \pm 2	1.32 \pm 0.04
potassium fixed	67.5 \pm 1.8	383 \pm 5	98 \pm 3	1.46 \pm 0.06
<u>hectorite</u>				
sodium form (105 $^{\circ}\text{C}$)	3.7 \pm 0.1	348 \pm 0	105 \pm 5	1.14 \pm 0.05
sodium form (220 $^{\circ}\text{C}$)	3.6 \pm 0.2	353 \pm 0	98 \pm 8	1.26 \pm 0.09
lithium fixed	4.0 \pm 0.2	353 \pm 0	97 \pm 8	1.28 \pm 0.10
potassium fixed	7.4 \pm 0.2	361 \pm 2	89 \pm 7	1.46 \pm 0.12
<u>nontronite</u>				
sodium form (105 $^{\circ}\text{C}$)	1.4 \pm 0.0	396 \pm 3	73 \pm 3	2.10 \pm 0.09
sodium form (220 $^{\circ}\text{C}$)	1.1 \pm 0.0	398 \pm 0	44 \pm 2	3.54 \pm 0.21
lithium fixed	0.9 \pm 0.0	343 \pm 5	90 \pm 0	1.30 \pm 0.03
potassium fixed	0.7 \pm 0.0	336 \pm 3	60 \pm 4	1.87 \pm 0.15

pounds (Marfunin, 1979, p. 255). For the clays studied, such vacancies would probably be few and confined to the samples exhibiting the lowest degree of crystallinity. The radical SiO_4^{5-} (*i.e.*, Si^{3+} or $\text{Si}^{4+} + e^-$) could be produced by ionizing radiation and stabilized by interstitial cations. Such radicals have been observed to exist in zircon and quartz (Marfunin, 1979, p. 264). Finally, substitution of trace amounts of Ti^{4+} for Al^{3+} in the octahedral layer was observed for all samples (Tables 4 and 5) (Jackson, 1975, p. 546). This substitution produces a lattice site of excess positive charge which would be neutralized by trapping a free electron.

The sodium samples prepared by heating at 220 $^{\circ}\text{C}$ demonstrate a reduced TL glow curve in comparison with the TL spectra of the sodium clays prepared at 105 $^{\circ}\text{C}$ (Table 7). The reduction of the TL signal observed for the hectorite clay is small, and within error, their intensities might be equal. Since the sodium samples prepared by heating at 105 $^{\circ}\text{C}$ serve as references demonstrating the number of naturally occurring traps and holes, the annealing effects of heating are displayed by the TL glow curve of the sodium samples heated at 220 $^{\circ}\text{C}$. For these samples then, this annealing reduces the number of traps and holes capable of participating in the TL process.

Cation fixation of the samples presents a marked change in the TL spectra of all the smectites and the hectorite. TL glow curves of lithium-fixed montmorillon-

ites are the most intense peaks for all montmorillonite samples (Table 7). This indicates that the fixation of cations provides an increase in the number of traps in the clay lattice. It appears as though these fixed lithium cations are themselves new electron traps, behaving as the compensator cations do in quartz, that is, accepting free electrons produced during irradiation and existing as Li° atoms in the crystal lattice (Marfunin, 1979, p. 255).

Potassium fixation also exhibits a similar phenomenon of increased TL intensity. The potassium-fixed montmorillonites have the second most intense TL signal, and the TL spectrum of the potassium-fixed hectorite is the most intense glow curve for all the hectorite samples. As with lithium-fixed samples, potassium cations appear to take on the role of electron traps when fixed to the oxygen surface of the clay, existing as K° after irradiation. Since potassium fixation is not as extensive as lithium fixation, the increase in TL intensity for the potassium fixed montmorillonites is not as great as it is for the lithium fixed montmorillonites. For hectorite, potassium fixation has a greater effect on the TL signal than does lithium fixation. This is to be expected though, since lithium fixation is not as great for hectorite as it is for the montmorillonites. The TL spectra of nontronite is essentially unaffected by either lithium or potassium fixation. If there is an effect, it serves to slightly reduce the intensity of the TL signals.

For the montmorillonites, there is a good correlation of the increase observed in the intensity of the TL signals for the cation fixed clays with the charge deficiencies of the unit cells calculated for these samples (Tables 5 and 8). The percentage increase in TL peak intensities in going from the sodium form of montmorillonites prepared at 105°C to the potassium-fixed forms is largest for samples with the greatest tetrahedral charge deficiencies (Table 5 and 8). Also, the percentage increase in the TL glow curve intensity in going from the sodium montmorillon-

ites prepared at 220°C to the lithium-fixed clays is greatest for the montmorillonites with the greatest total charge deficiencies (tetrahedral and octahedral charge deficiencies), (Tables 5 and 8). The intensity of a TL glow curve for a cation fixed montmorillonite depends not only on the total number of charge deficiencies, but also on their location in the crystal lattice and the type of cation fixed with the clay. For example, a potassium cation fixed to the surface of a clay due to a charge deficiency located in the tetrahedral layer may receive the free electron released by this defect during irradiation forming K° . However, a potassium ion fixed to a clay due to an octahedral charge deficiency may be too loosely bound to receive the free electron this defect released. Potassium cations fixed due to octahedral substitutions are bound to the clay with less energy than potassium fixation due to tetrahedral defects (van Olphen, 1977, p. 69). The ability of the potassium cations of lower fixation energy to rehydrate is believed to be the reason these cations are not able to trap electrons and participate in the TL process. It is difficult to believe that a K° atom could exist in the presence of interlayer water; therefore, the ability of a potassium to trap an electron seems to be related to its energy of fixation, which depends in turn upon the location of the defect responsible for its fixation. This is not always true since Texas montmorillonite exhibits a fairly large increase in TL signal intensity in going from its sodium form prepared at 105°C to its potassium fixed form. The Texas clay does have a moderately high octahedral substitution which may bind some potassium cations with enough energy to allow for electron capture.

With regards to lithium fixation within the samples, which is capable of occurring by migration into both tetrahedral and octahedral layers, (Calvet and Prost, 1971) the fixed lithium cation will be able to exist closer to the charge deficiency responsible for its fixation. The lithium cation would be close enough to the defect and

Table 8. TL glow curve intensity increase in going from sodium to cation fixed forms, and sample charge deficiencies

Sample	Increase in TL intensity in going from sodium form (105°C) to potassium fixed form. (%)	Increase in TL intensity in going from sodium form (220°C) to lithium fixed form (%)	Tetrahedral charge deficiency (eq.)	Octahedral charge deficiency (eq.)	Total charge deficiency (eq.)
Wyoming montmorillonite	96.8	152.0	0.61	0.43	1.04
Texas montmorillonite	38.2	72.7	0.03	0.64	0.67
Arizona montmorillonite	90.7	365.0	0.45	0.98	1.43
hectorite	100.0	11.1	0.26	1.19	1.45
nontronite	-50.0	-18.1	1.14	0.21	1.14

possess sufficient fixation energy as to easily trap most electrons released producing a stable Li° atom.

For all the montmorillonites and the hectorite samples, the average energies of the traps produced by potassium fixation are higher in value than the existing natural traps or those traps produced by lithium fixation (Table 7). Within experimental error, the values of the activation energies of the two sodium forms treated at 105° and 220°C and lithium fixed samples are equal for a given clay. It can be concluded that heating and lithium fixation do not appreciably affect the average activation energies of the electron traps of these clays. In most cases though, both heating and cation fixation (lithium or potassium) reduces the maximum temperature of the TL glow curve of a sample and reduces the half-width of the peak at its half-height. This half-width reduction indicates that heating and cation fixation reduce the range of electron trap activation energies of a given sample, producing more uniform activation energies (Table 7).

Nontronite exhibited TL spectra inconsistent with all the other clays investigated. The TL spectra of nontronite did not reflect its octahedral charge deficiency while the other samples demonstrated an increase in TL glow curve intensity with increasing octahedral charge deficiency. Also, cation fixation did not produce an increase in the TL spectra of nontronite as it did in the other samples. Its trioctahedral–dioctahedral properties may account for this observation. However, it is believed that the high concentration of iron in this sample is responsible for this behavior. Quenching of the TL signal by the presence of iron could reduce the TL intensity of the nontronite to such an extent as to make interpretation impossible (Medlin, 1968).

Conclusions

The results obtained for the unheated clay minerals in their sodium-exchanged form indicate that the TL glow curve intensities are proportional to the extent of octahedral layer charge deficiency. Trapped holes are proposed as existing at an oxygen which bridges an octahedron with a charge deficient octahedron. Charge deficiency may arise from the substitution of a cation with a cation of lower valence or a cation vacancy. Extensive cation vacancies in the octahedral layer of dioctahedral clays causes greater TL de-excitation curve intensities from these clays as compared to trioctahedral clays. Naturally occurring electron traps in clays are caused by anion vacancies, the formation of the SiO_4^{5-} radical, and Ti^{4+} substitution for Al^{3+} developing a lattice site of excess positive charge.

Annealing, caused by heating a sample prior to exposure to radiation, alters the number of electron-hole centers capable of forming in a clay thereby reducing the intensity of a TL glow curve.

Cation fixation introduces new electron traps (Li° and K°) into the crystal lattice causing an increase in TL

intensity. The percentage increase in the number of electron-hole centers formed in going from the sodium-exchanged form of the clay to its potassium-fixed form is proportional to the degree of tetrahedral charge deficiency. This percentage increase is proportional to the total charge deficiency of a clay for lithium fixation. The average relative electron trap activation energies are highest for potassium fixed clays. Cation fixation and heating a clay lower the temperature and half-width of its TL de-excitation curve.

These above-mentioned observations are true for the montmorillonites investigated and, in general, for the hectorite sample. Nontronite demonstrates deviations from these observations which are likely due to excessive quenching of the TL signal by iron, thereby reducing the sensitivity of the TL de-excitation curve for nontronite.

Acknowledgments

The authors would like to thank Southern Clay Company, Inc. and The Robert A. Welch Foundation for financial support.

References

- Aitken, M. J. (1974) *Physics and Archaeology*. Clarendon Press, London.
- Braunlich, P. (1968) Thermoluminescence and thermally stimulated current—tools for determination of trapping parameters. In D. J. McDougall, Ed., *Thermoluminescence of Geological Materials*, p. 61–88. Academic Press, New York.
- Calvet, R. and Prost, R. (1971) Cation migration into empty octahedral sites and surface properties of clays. *Clays and Clay Minerals*, 19, 175–186.
- Grim, R. E. (1968) *Clay Mineralogy*. McGraw-Hill, Inc., New York.
- Jackson, M. L. (1975) *Soil Chemical Analysis—Advanced Course*. Published by the author, Madison, Wis.
- Lemons, K. and McAtee, J. L., Jr. (1982) Induced thermoluminescence of some clay minerals. *Clays and Clay Minerals*, 30, 311–314.
- Marfunin, A. S. (1979) *Spectroscopy, Luminescence, and Radiation Centers in Minerals*. Springer-Verlag, New York.
- Medlin, W. L. (1968) The nature of traps and emission centers in thermoluminescent rock materials. In D. J. McDougall, Ed., *Thermoluminescence of Geological Materials*, p. 193–223. Academic Press, New York.
- Mehra, O. P. and Jackson, M. L. (1959) Iron oxide removal from soils and clays by a dithionite–citrate system buffered with sodium bicarbonate. *Clays and Clay Minerals*, 7, 317–327.
- Ralph, E. K. and Han, M. C. (1968) Progress in Thermoluminescent dating of pottery. In D. J. McDougall, Ed., *Thermoluminescence of Geological Materials*, p. 379–387. Academic Press, New York.
- van Olphen, H. (1977) *An Introduction to Clay Colloid Chemistry*. John Wiley and Sons, Inc., New York.
- van Olphen, H. and Fripiat, J. J. (1979) *Data Handbook for Clay Minerals and Other Nonmetallic Minerals*. Pergamon Press, Elmsford, New York.